Reflectance variation in boreal landscape during the snow melting period using airborne imaging spectroscopy

Heinilä, Anna Maaria Kirsikka

2019-04

Heinilä , A M K , Salminen , M , Metsämäki , S , Pellikka , P K E , Koponen , S & Pulliainen , J 2019 , ' Reflectance variation in boreal landscape during the snow melting period using airborne imaging spectroscopy ' , International Journal of Applied Earth Observation and Geoinformation , vol. 76 , pp. 66-76 . https://doi.org/10.1016/j.jag.2018.10.017

http://hdl.handle.net/10138/298713
https://doi.org/10.1016/j.jag.2018.10.017

Int J Appl Earth Obs Geoinformation 76 (2019) 66–76

Contents lists available at ScienceDirect

Int J Appl Earth Obs Geoinformation

journal homepage: www.elsevier.com/locate/jag

Reflectance variation in boreal landscape during the snow melting period using airborne imaging spectroscopy

Kirsikka Heinilä[a,*], Miia Salminen[b], Sari Metsämäki[a], Petri Pellikka[c,d], Sampsa Koponen[a], Jouni Pulliainen[b]

[a] Finnish Environment Institute, Latokartanonkaari 11, 00790 Helsinki, Finland
[b] Finnish Meteorological Institute, P.O. Box 503, FI-00101 Helsinki, Finland
[c] College of Global Change and Earth System Science, Beijing Normal University, 1000875 Beijing, China
[d] Department of Geosciences and Geography, University of Helsinki, P.O. Box 64, FI-00014 Helsinki, Finland

ARTICLE INFO

Keywords:
Reflectance
AISA
Spectroscopy
Scene reflectance
Snow melt
NDSI
NDVI
Boreal forest
Land cover classification
Fell
Snow mapping
FSC
SCE
MODIS

ABSTRACT

We aim a better understanding of the effect of spring-time snow melt on the remotely sensed scene reflectance by using an extensive amount of optical spectral data obtained from an airborne hyperspectral campaign in Northern Finland. We investigate the behaviour of thin snow reflectance for different land cover types, such as open areas, boreal forests and treeless fells. Our results not only confirm the generally known fact that the reflectance of a melting thin snow layer is considerably lower than that of a thick snow layer, but we also present analyses of the reflectance variation over different land covers and in boreal forests as a function of canopy coverage. According to common knowledge, the highly variating reflectance spectra of partially transparent, most likely also contaminated thin snow pack weakens the performance of snow detection algorithms, in particular in the mapping of Fractional Snow Cover (FSC) during the end of the melting period. The obtained results directly support further development of the *SCAmod* algorithm for FSC retrieval, and can be likewise applied to develop other algorithms for optical satellite data (e.g. spectral unmixing methods), and to perform accuracy assessments for snow detection algorithms.

A useful part of this work is the investigation of the competence of Normalized Difference Snow Index (NDSI) in snow detection in late spring, since it is widely used in snow mapping. We conclude, based on the spectral data analysis, that the NDSI -based snow mapping is more accurate in open areas than in forests. However, at the very end of the snow melting period the behavior of the NDSI becomes more unstable and unpredictable in non-forests with shallow snow, increasing the inaccuracy also in non-forested areas. For instance in peatbogs covered by melting snow layer (snow depth < 30 cm) the mean NDSI -0.6 was observed, having coefficient of variation as high as 70%, whereas for deeper snow packs the mean NDSI shows positive values.

1. Introduction

A notable issue in optical remote sensing of snow cover is the problem of snow detection in spatially heterogeneous landscapes at the end of the melting season when a signal can be affected by snow-covered ground, snow-free ground and tree canopy (Dietz et al., 2012; Frei et al., 2012; Vikhamar and Solberg, 2003b; Xin et al., 2012). Some studies on the reflectance or albedo from snow-covered forests exist, but typically they do not consider melting snow conditions with a thin partially transparent snow (e.g. Canisius and Chen, 2007; Webster and Jonas, 2018). On the other hand, e.g. Dozier et al., (2009); Negi et al. (2010); Singh et al. (2010) and Shekhar et al. (2018) investigate the effect of grain size, snow wetness and snow depth on the visible (VIS) and near-infrared (NIR) reflectance during the melting process but focus only on non-forested areas. In some investigations the scene reflectance from boreal landscape during full snow cover has been successfully modelled, *e.g.* by Vikhamar and Solberg (2003a), Niemi et al. (2012) and Pulliainen et al. (2014). However, both the modelling experiments and experimental data analysis lack the consideration of thin and dirty snow layers as well as the high variability of snow depth from snow-free ground patches to thicker snow packs, which is typical to boreal forests. In this work we tackle these questions by investigating the variability of the melting snow and snow-free ground reflectance with focus on the boreal forest zone with detailed information on the

* Corresponding author.
E-mail address: kirsikka.heinila@environment.fi (K. Heinilä).

https://doi.org/10.1016/j.jag.2018.10.017
Received 6 July 2018; Received in revised form 19 October 2018; Accepted 25 October 2018

Table 1
The description of the utilized datasets and the applications.

Dataset/ Measurement Cases	Orig. resolution	Regridded	Method	Application
AISA 80 cm airborne reflectances Measurement cases: 1) Sodankylä 5 May 2011: *sd* < 30 cm, cloud cover 0/8, Sun elevation angle 27°, T 5 °C 2) Sodankylä 18 March 2010: *sd* > 70 cm, cloud cover 0/8–2/8, Sun elevation angle 22°, T −4 °C 3) Saariselkä 5 May 2011: *sd* < 60 cm, cloud cover 7/8, diffuse illumination, T 4 °C*	80 × 80 cm^2	NA	NA	AISA reflectances or indices for different CLC2012 classes –Measurement Case 1 (see Section *3.1*) and Case 3 (see Section *3.2*) Airborne reflectance compared with the indicative ground-based target reflectances –Measurement Case 1 and Case 2 (see Section *3.3*)
AISA 10 m airborne reflectances Measurement Cases 1), 2) and 3) as in AISA 80 cm reflectances	80 × 80 cm^2	10 × 10 m^2	- filtered with mean filter using a 12 × 12 window for 80 cm AISA data - resampling with the nearest neighbour method	AISA reflectances or indices for different Canopy Cover classes –Measurement Case 1 (see Section *3.1*), Case 2 (see Section *3.1*), and 3 (see Section *3.2*) Performance of NDSI in snow mapping –Measurement Case 1 (see Section *3.1*) and Case 3 (see Section *3.2*)
ASD field spectroscopy Reflectances from a spectral database	0.1 m^2	NA	NA	Airborne reflectance compared with the indicative ground-based target reflectances (see Section *3.3*)
CLC2012 Corine Land cover map	20 × 20 m^2	80 × 80 cm^2	- resampling with the nearest neighbour method	AISA reflectances or indices for different CLC2012 classes (see Sections *3.1* and *3.2*)
Canopy Cover (CC) derived from LIDAR measurements	10 × 10 m^2	NA	NA	Behaviour of AISA reflectances or indices in different Canopy Cover classes (see Sections *3.1* and *3.2*)

* 2 m air Temperature measured at FMI-ARC.

canopy closure associated with each reflectance observation.

During the spring snow melt the snow layer is rather heterogeneous with respect to the spatial distribution, snow depth, grain size, density and albedo; this is due to the differences in snow accumulation followed by the varying melt rates driven by several forcing effects such as micrometeorology, topography, snow soot contamination and forest canopy density (Clark et al., 2011; Davis et al., 1997; Molotch et al., 2016; Varhola et al., 2010). In late spring, the snow grains are metamorphosed and snow is moist or wet. The increasing effective grain size, related to the increasing snow wetness, decreases reflectance in the NIR region (Warren, 1982; Singh et al., 2010). Apart from those, the thinning snow layer comes more transparent and the vegetation under the snow emerges through the snow layer.

Vegetation typically has a low reflectance in the visible spectral region because of its strong absorption properties, whereas snow has a very high reflectivity. The impurities, which are accumulated on the snow surface as a consequence of upper snow layer springtime melt, decrease snow reflectance and albedo at visible wavelengths, but have only a negligible effect on the near-infrared wavelengths > 900 nm (e.g. Grenfell et al., 1981; Warren and Wiscombe, 1980). Thus, during the melting period particularly, the visible reflectance of snow-covered landscape gradually decreases when the snow layer gets thinner and finally melts off revealing the ground underneath.

We organized an airborne imaging spectroscopy campaign in Northern Finland in May 2011 in order to investigate the behaviour of terrain reflectance, Normalized Difference Snow Index (NDSI) and Normalized Difference Vegetation Index (NDVI) near the end of the snowmelt period. We also investigated the effect of Canopy Cover (CC) on the reflectance and on the indices for ground covered by thin melting snow layer. Additionally, we demonstrated the performance of the widely utilized NDSI (Frei et al., 2012; Hassan et al., 2012; Lin et al., 2012; Panday et al., 2014; Riggs et al., 2017; Steele et al., 2017; Xin et al., 2012) to detect snow for different land cover types and under melting snow conditions. Using mast-borne spectrometer data, Niemi et al. (2012) investigated the feasibility of MODIS MOD10_L2 binary and fractional snow products (FSC) of Collection 5 (C5) (Hall et al., 1998; Klein et al., 1998; Riggs et al., 2006) in the study site used also the present work. Heinilä et al. (2014) repeated this investigation using airborne data under thick dry snow pack conditions. Here, we continue this work with the airborne spectrometer data representing melting snow conditions and taking into account the recent revisions in MODIS Collection 6 (C6) (Riggs et al., 2016).

The aim of this paper is to provide information on reflectance variation in boreal landscape at the very end of the melting period when the snowpack is thin. This research supports the development work of *SCAmod* –method (Metsämäki et al., 2012, 2005; Pulliainen et al., 2014), a method currently used in various regional and hemispherical snow services providing information on FSC (also denoted as SCE or SCA), introduced by (Metsämäki et al., 2015; Nagler et al., 2015; Schwaizer and Ripper, 2017).

2. Material and methods

2.1. Study area and measurement conditions

The study area is composed of two sites: Sodankylä and Saariselkä, both located in the boreal and subarctic regions in Northern Finland. The Sodankylä boreal forest study site encircles the Arctic Space Centre of the Finnish Meteorological Institute (FMI-ARC) at 26.6 °E 67.4 °N, about 100 km north of the Arctic Circle and 180 m above sea level. The other study site is at Saariselkä, 28.2 °E 68.3 °N, 200 km north of the Arctic Circle. Saariselkä is a fell area (highest point 718 m above sea level) consisting of mires, boreal forests and heathlands and with a timberline at an altitude of 400 m above sea level (higher altitudes representing fell tundra).

In Northern Finland, the melting season usually starts at the end of

Fig. 1. Snow conditions during the campaign on 5 May 2011 in Sodankylä. Snow patches represent snow depths within the range]0, 30] cm.

Fig. 2. RGB true colour images applying red (640 nm), green (552 nm) and blue (462 nm) bands, Sodankylä on 5 May 2011. During the data acquisition ground was partially snow-covered. In the background there is an ortophoto by the National Land Survey of Finland from summer time conditions (For interpretation of the references to colour in this figure legend, the reader is referred to the web version of this article).

April. At the time of the campaign (5 May 2011) snow cover was melting and the land surface was partially snow-free. In snow-covered areas snow depth *sd* was]0, 30] cm at the Sodankylä site and]0, 60] cm at the Saariselkä site implying that the spring melt was clearly more advanced in Sodankylä. Additionally, more snow-free patches were found at Sodankylä than Saariselkä (Table 1). During the measureemnts the sky was cloudless in Sodankylä having the solar elevation 26°–30° and cloudy (cloud cover 7/8) in Saariselkä. Figs. 1 and 2 depict the conditions in Sodankylä and Fig. 3 in Saariselkä during the campaign day on 5 May 2011. The forests at both sites are dominated by Scots pine (*Pinus silvetris*) and typical undergrowth species are heather (*Calluna vulgaris*), lingonberry (*Vaccinium vitis-idaea*), reindeer lichens (*Cladonia* spp.) and mosses (e.g. *Pleurozium schreberi*). Additionally, the snow-free ground right after snow clearance contains e.g. rocks, twigs and dead plants such as leaves, needles and hay. The rocks at both study sites belong to the Metamorphic rocks. During the campaign days, typically for the season, there is no snow on forest canopy; accordingly, we refer to sub-canopy snow when discussing the snow in forests. Images from snow cover and snow-free ground on 5 May 2011 are presented in Supplementary Data (SD1 and SD2).

2.2. Material

2.2.1. Spectrometer data

The airborne hyperspectral data were acquired with an AisaDUAL imaging spectrometer manufactured by Spectral Imaging Ltd (SPECIM). The instrument combines the AisaEAGLE and AisaHAWK sensors for simultaneous acquisition of VNIR and SWIR data. The details of the instrument set-up are described in Supplementary Data (SD3). We used the Oxford Technical Solutions RT4000 GPS/IN to provide high accuracy position measurements with low drift rates. The reflectance level was obtained by applying a real-time fibre optic downwelling irradiance sensor (FODIS). Segments of the flight lines on 5 May 2011 are shown in Fig. 2 and in Fig. 3 of Sodankylä and Saariselkä, respectively. More details of the flight lines and flight conditions are shown in Supplementary Data (SD4). In addition to the principal campaign day, the airborne AISA data from the Sodankylä site, but on different day (18 March 2010), is utilized in order to provide reference data representing full snow conditions. During that data acquisition the ground was covered by an over 70 cm deep, dry snow layer and the sky was cloud-free. These data are described in more detail in Heinilä et al. (2014).

In addition to the airborne spectrometer data, indicative field spectrometer data measured with Analytical Spectral Devices (ASD) Field Spec Pro JR was utilized in the investigation. The ASD measurements are from a spectral database maintained by the Finnish Environment Institute and the Finnish Meteorological Institute. This spectral database is a collection of numerous reflectance spectra from different targets and under different conditions measured in the several campaigns (see details in Salminen et al., 2009).

2.2.2. Corine land cover 2012 data

Corine Land Cover 2012 (CLC2012) data production is a part of the Copernicus program. CLC12 for Finland was produced by integrating automatically interpreted satellite images and spatial datasets resulting in a raster database with a pixel size of 20 by 20 m (Härmä et al., 2015; Törmä et al., 2011). In this investigation we utilized the most common CLC12 land cover classes at the study sites. These land cover types mainly consist of coniferous forests and open areas on mineral soil, but there are also peatbogs. The proportions of utilized land cover types in study sites, as well as in the Sodankylä municipality, are included in the Supplementary Data (SD5).

2.2.3. LIDAR data for forest canopy characteristics

Airborne Laser Scanning (ALS) data provided by the National Land Survey (NLS) of Finland was used to create Canopy Cover (CC) maps for

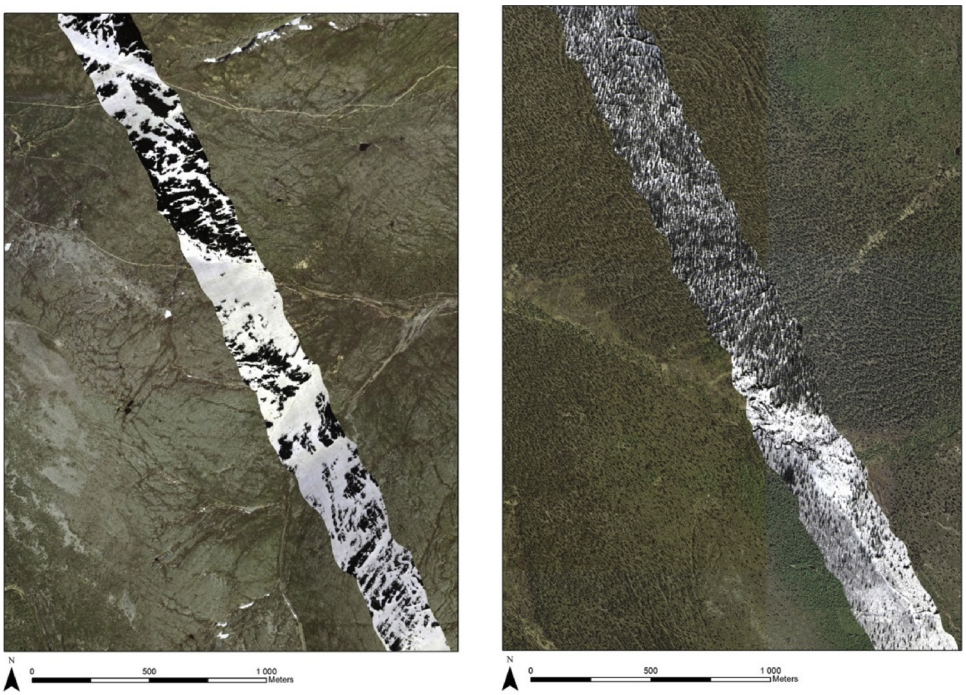

Fig. 3. RGB true colour images, applying red (640 nm), green (552 nm) and blue (462 nm) bands, of the section of the first AISA flight line (left) and the second AISA flight line (right). During the data acquisition the ground was partially snow-covered. In the background there is an ortophoto by National Land Survey of Finland from summer time conditions (For interpretation of the references to colour in this figure legend, the reader is referred to the web version of this article).

grid cells of 10 × 10 m^2. The LIDAR (Light Detection and Ranging) scanning was performed in May 2010 in the Sodankylä and Saariselkä areas, when deciduous trees were leafless. The utilized LIDAR data are described in more detail in Cohen et al. (2015). In this investigation we utilized the data set to study the effect of CC on the reflectances and indices during the snowmelt period.

2.3. Data processing methods

The AISA data were radiometrically and geometrically corrected using the SPECIM's CaliGeo tool of the ENVI software. Measurements from Saariselkä were also corrected with the digital elevation model KM10 by the National Land Survey with a pixel size of 10 × 10 m^2 and elevation resolution of 1.4 m. The investigation of the AISA data focused on certain bands consistent with the Moderate Resolution Imaging Spectroradiometer (MODIS) onboard Terra satellite. The extraction of the corresponding MODIS bands (Band 1: 645 nm; Band 2: 858.5 nm; Band 4: 555 nm; Band 6: 1640 nm) from AISA spectra was carried out by using the band specific FWHM (full width at half maximum) criterion. For easy readability, we use the same naming convention for AISA bands (i.e. bands 1–6) as for MODIS bands. The CLC2012 data originally in a 20 × 20 m^2 grid was resampled using the nearest neighbour method to match with the 80 cm spatial resolution of the AISA imagery. To be compatible with the CC data, the AISA lines from Sodankylä and Saariselkä were first resampled with a mean filter using a 12 × 12 window corresponding to pixel size of 10 × 10 m^2 and then re-projected to the corresponding grid. The data sets and their applications are shown in Table 1.

2.4. Data analysis methods

From the airborne AISA reflectance data we derived the NDSI (Band 4 – Band 6) / (Band 4 + Band 6) and the NDVI (Band 2 – Band 1) / (Band 2 + Band 1). The behaviour of reflectance in bands 1–6 and the indices were investigated for different CLC2012 classes with the 80 cm pixel size. At the time of the field campaign, the land was only partially covered by snow. We extracted the areas of snow-free ground (sd = 0 cm) and snow-covered ground from the Sodankylä and Saariselkä datasets based on visual interpretation. The snow-covered forest pixels near the very end of the melting period may contain snow-free patches *e.g.* around the trees, but we aimed to exclude these using manual interpretation. The Supplementary Data (SD5) describe the utilized land cover classes and the number of observed pixels at the Sodankylä and Saariselkä sites. The mean μ, standard deviation σ and coefficient of variation CV were calculated for all the investigated CLC12 classes:

$$CV = \frac{\sigma}{|\mu|} \times 100\,\% \tag{1}$$

The actual change ΔOBS and the relative change ΔOBS_{REL} between the snow-covered and snow-free reflectances or indices were utilized in the investigation and were calculated as follows:

$$\Delta OBS = \langle OBS_S \rangle - \langle OBS_{SF} \rangle \tag{2}$$

$$\Delta OBS_{REL} = \frac{\Delta OBS}{OBS_{SF}} \times 100\% \tag{3}$$

where OBS_S = reflectance or index observed for snow-covered ground
OBS_{SF} = reflectance or index observed for snow-free ground.

We compared the AISA data with a Canopy Cover map (CC) derived from LIDAR measurements. The CC data were divided into 11 equal interval class of 10%-units 0–5%, 5–15%, 15–25%,…85–95%, 95–100%. The mean and standard deviation of reflectances and indices were calculated for these intervals. Exponential regression lines between CC and reflectances as well as linear regression lines between CC and indices are provided. The AISA data from March 2010 was utilized to investigate the differences in the relation of CC and reflectances or indices between the two snow conditions: 1) ground covered by a dry over 70 cm snow layer in March 2010 and 2) ground covered by a melting snow layer, 0 cm < sd < 30 cm, in May 2011.

In addition, we investigated the competence of NDSI in snow mapping during the melting period. In practice, to demonstrate the feasibility of NDSI_Snow_Cover product from MODIS Collection 6 (C6), we depicted AISA data for different land cover types showing the C6 limits for Band4 and NDSI utilized in NDSI_Snow_Cover to predict snow (Riggs et al., 2016). In this analysis, observations were collected from study sites featuring different canopy coverages. The 10 × 10 m^2 AISA data were used instead of 80 cm resolution to obtain observations from the whole forest stand (not from a single tree crown).

We also identified manually the directly illuminated snow areas

from the Sodankylä AISA imagery. The AISA reflectances of these areas were compared with observations made with ASD field spectrometer from the thin melting snow layer under direct illumination. Additionally, the AISA reflectances of thin melting snow layer were compared with (1) AISA reflectances observed for dry over 70 cm deep snow layer, (2) with ASD reflectances of moss, lingonberry and lichen measured on late spring right after snow measurement and (3) with ASD reflectance of pine branch measured with a laboratory setup.

3. Results

3.1. AISA –derived quantities under direct illumination from various land cover types at Sodankylä

We examined the reflectances, their related indices, and other quantities described in Section 2.4 of snow-covered and snow-free ground for Sodankylä site characterized by patchy thin]0, 30] cm snow layer under direct illumination. According the analyses, the CVs in the near-infrared and shortwave infrared wavelengths were rather similar for snow-covered and snow-free ground, but in the visible region the CV was at least twice as high for the former. Overall, the highest relative change between the land cover stratified reflectances from snow-covered and snow-free ground was observed at green wavelengths (555 nm), providing a mean relative change of 140%. At 555 nm the relative reflectance change was highest (254%) in the peat-mining area, which is explained by the lack of vegetation and the strong contrast between white snow and dark peat (Fig. 4). The second highest relative reflectance change (172%) was found for the transitional woodland/shrub (cc < 10%) and the third highest for peatbogs (165%) (Fig. 4). The lowest relative reflectance change (84%) was observed for the broad-leaved forest on peatland. For shortwave infrared (1640 nm) the transition from thin snow layer to snow-free ground induces both positive and negative changes in reflectance (Fig. 4). Apparently the direction and magnitude of changes are dependent on land cover class. For instance, 1640 nm reflectance change on mineral land is strongly negative while on peatland the change is mostly positive.

The quantities reported above are given for all the measured wavelengths in the Supplementary Dataset (SD6).

Our investigations on the behavior of NDSI for different CLC2012 classes show that NDSI in snow-covered areas is considerably different for different land covers; for instance the mean NDSI for Transitional woodland/shrub, cc 10–30%, on rocky soil is -0.11 while NDSI is for Peatbogs -0.55. However for certain classes also the class-specific internal variation was high. For the entire dataset i.e. for all CLC-classes with thin snow layer, the mean NDSI and CV was –0.44 and 150%, correspondingly. Remarkably, CC-stratified mean NDSI was negative even with a CC < 5% (Fig. 5). For snow-free terrain, the mean NDSI for all CLC2012 classes was –0.77 with CV of 13%. In contrast to NDSI, NDVI was found to be a more stable index, having a mean value of 0.53 and CV of 15% for snow-free ground and a mean value of 0.41 and CV of 55% for thin snow.

Fig. 5 presents the green and NIR reflectances as well as NDSI and NDVI for thick ($sd > 70$ cm) dry snow and thin melting snow ($sd <$ 30 cm) as function of Canopy Cover (CC). According the figure, NDSI and NDVI correlated rather linearly with the CC while correlation between CC and reflectances was more exponential than linear; however this exponential relation is more pronounced for dry snow. In the case of NIR band, the reflectance stays about the same for CC of 60–100%. The standard deviations of NDSI and NDVI are distinctively different for dry snow and thin melting snow, whereas the standard deviations of reflectances are somewhat similar independently of snow conditions. In Fig. 5 as well as in Fig. 8, the values related to CC are placed at the central values of the invidual intervals.

Fig. 6 presents all observations from the Sodankylä site, processed to 10×10 m^2 pixel size, in NDSI–Band 4 space with the thresholds of MODIS Collection 6 (C6) MOD10_L2 NDSI_Snow_Cover product to detect snow (Riggs et al., 2016). In the NDSI_Snow_Cover product a pixel with NDSI > 0.0 is considered to have some snow present. Pixels detected with snow cover in the 0.0 < NDSI < 0.10 are reversed to a 'not snow' result and bit 2 of the NDSI_Snow_Cover_Algorithm_Flags_QA is set. If the visible reflectance from MODIS band 2 ≤ 0.10 or band 4 ≤ 0.11 then a pixel fails to pass Low VIS reflectance screen, and results in "no decision" (Riggs et al., 2016). When AISA observations were placed into the NDSI − Band 4 space, many of the observations from snow-covered ground were interpreted as snow-free (Fig. 6). The threshold of 0.0 for NDSI (see Section 2.4) detected only 22% of the snow-covered cases when CC ≥ 10%. Even in non-forests (CC < 10%) 55% of the snow-covered pixels had a negative NDSI value in the study area. Additionally, it is evident that snow-covered areas can also have Band 4 reflectance lower than 0.11; this occurred for a notable portion of all the snow-covered cases (76% for CC ≥ 10% and 39% for CC < 10%) (Fig. 6). Band 2 reflectance was lower than 0.1 for 4% of the snow-covered cases where CC ≤ 10% and 12% of the snow-covered cases where CC > 10%. According to the MODIS NDSI_Snow_Cover data array, these cases would be labelled as 'snow-free' or "no decision". In case of snow-free observations, C6 MOD10_L2 NDSI_Snow_Cover performed very well and only few pixels with snow-free ground were classified as snow-covered.

3.2. AISA –derived quantities under diffuse illumination from various land cover types at Saariselkä

On the campaign day 5 May 2011, the behaviour of spring time AISA reflectances, NDSI and NDVI were investigated also in the Saariselkä fell area, where the spring snow melt takes place later than at Sodankylä. Due to this delay, snow-free areas were found only in three CLC2012 classes (moors and heathland, transitional woodland/shrub with canopy cover less than 10% and bare rock). At Saariselkä, the measurements were made under diffuse illumination, cloud cover 7/8, yielding to absence of shadows. The results from the direct illumination case (Sodankylä, see Fig. 5) are also depicted in this section to point out the effect of illumination conditions on the observed reflectances and indices.

For the snow-covered areas the behaviour of reflectance and their related indices was investigated for three CLC2012 classes (moors and heathland, transitional woodland/shrub with canopy cover less than 10% and bare rock); see Fig. 7. We found that visible and NIR reflectances were clearly highest over moors and heathlands. Also the highest NDSI and lowest NDVI were found that class. However, the mean NDSI was high for all of the three investigated CLC2012 classes (0.79–0.81). Additionally for NDSI the mean CV of 26% for CLC2012 classes was much lower than in Sodankylä study site (sd < 30 cm, direct illumination) where the mean NDSI was 150%. However, the relative change ΔOBS_{REL} was most distinctive at green wavelengths for all the investigated CLC2012 classes in green wavelengths, being as high as 1400% for moors and heathland, 870% for transitional woodland/shrub with canopy cover less than 10% and 870% for bare rock. For the snow-free areas, reflectance and indices behaved quite similarly for all of the three investigated CLC2012 classes, as indicated by Fig. 7. Finally, for those classes, the reflectances and their derived quantities are listed for all applied wavelengths in the Supplementary Dataset, see SD7.

For Saariselkä fell we also investigated the correlation between the Canopy Cover (CC) and i) the reflectances ii) NDSI and NDVI. The visible reflectances in Saariselkä were up to six times higher in dense forests (high CC) than in the Sodankylä direct illumination case (Fig. 8). Additionally, Fig. 8 shows that the visible reflectances were notably higher in Saariselkä also in open areas (low CC). We noticed that analogously to the direct illumination, the relationship between the CC and the reflectance was more exponential than linear also in diffuse illumination conditions. MODIS C6 MOD10_L2 NDSI_Snow_Cover criteria detected nearly all of the snow-covered AISA observations from

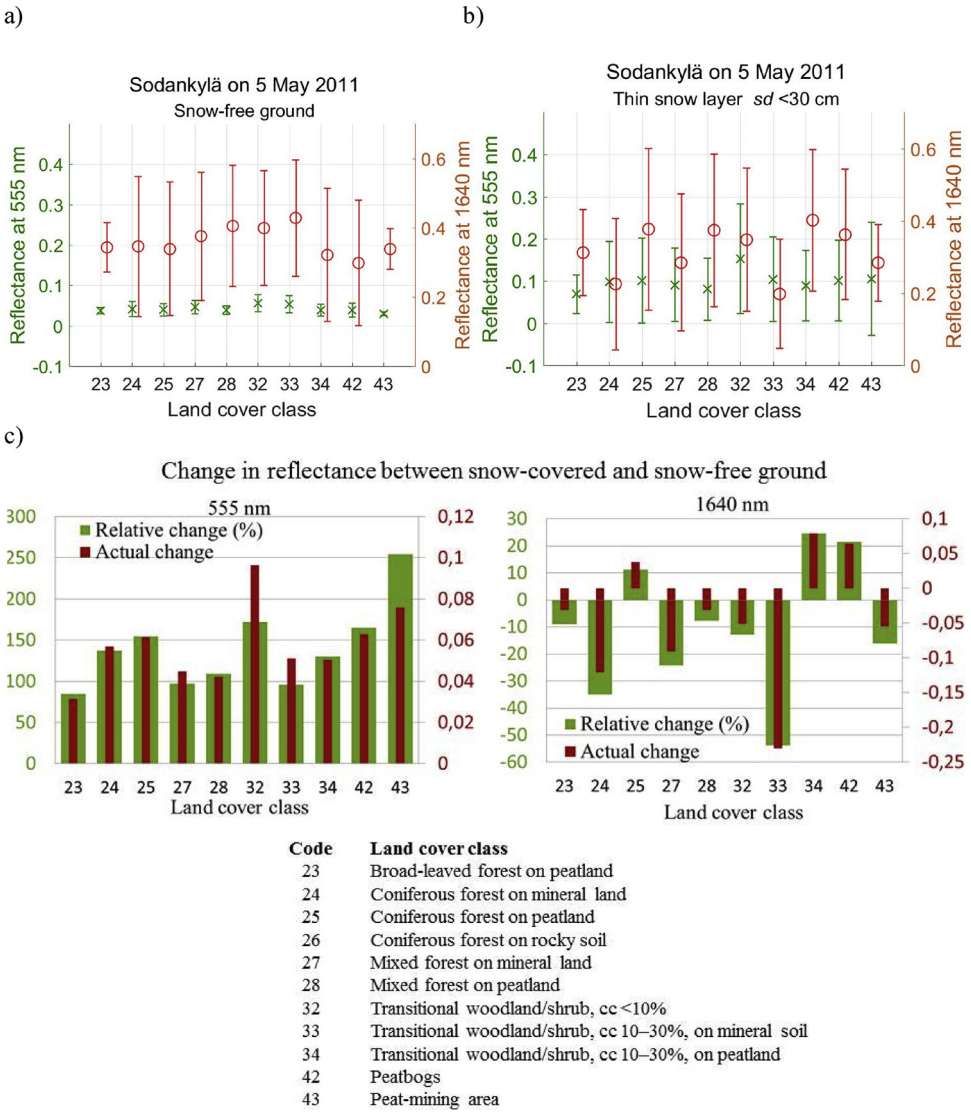

Code	Land cover class
23	Broad-leaved forest on peatland
24	Coniferous forest on mineral land
25	Coniferous forest on peatland
26	Coniferous forest on rocky soil
27	Mixed forest on mineral land
28	Mixed forest on peatland
32	Transitional woodland/shrub, cc <10%
33	Transitional woodland/shrub, cc 10–30%, on mineral soil
34	Transitional woodland/shrub, cc 10–30%, on peatland
42	Peatbogs
43	Peat-mining area

Fig. 4. Mean and standard deviation of reflectances at 555 nm (crosses) and 1640 nm (circles) from a) snow-free areas, b) areas covered by a melting snow layer (0 cm < *sd* < 30 cm), and c) the actual change ΔOBS (2) and relative change ΔOBS_{REL} (3) between these two cases for different CLC2012 classes at 555 nm and at 1640 nm. Analyses are based on the airborne 80 × 80 cm^2 AISA data from Sodankylä test site on 5 May 2011 under direct illumination.

Saariselkä under diffuse illumination (Fig. 9).

3.3. Behaviour of airborne reflectance compared with the indicative at-ground target reflectances

The AISA reflectances from the directly illuminated thin melting snow layer (*sd* < 30 cm) were compared with the measurements made using the ASD field spectrometer from thin melting snow layer of varying depth under direct illumination, Fig. 10. In visible wavelengths, AISA measurements were notably lower than the ASD measurements. In NIR region, AISA and ASD produced similar values, but in the 1200–1800 nm region, AISA measurements were higher than ASD measurements. Overall, the AISA reflectances, compared to ASD ground based measurements, are closer to the reflectances of vegetation. Fig. 10 also depicts the effect of snow depth (*sd*) on the ASD reflectances for *sd* of 24 cm, 15 cm, 9 cm and 7 cm. These measurements were made at the same location within 30 min and under direct sunlight. The reflectance was nearly the same at *sd* = 15 cm and *sd* = 24 cm, but at *sd* = 9 cm and *sd* = 7 cm it was notably lower in the visible region. In the NIR region, there were no notable differences between different snow depths.

4. Discussion

The analysis of AISA reflectances under direct illumination in various land cover types during the snow melting indicates that in visible wavelengths the variability of reflectance is clearly higher for snow-covered ground compared to snow-free ground. In contrast to that the variability at infrared region (both NIR and SWIR) is relatively low and practically independent on the presence of snow, see Fig. 4 and Supplementary Data (SD6). The high variation of visible reflectance is most likely caused by the variation in snow depth (thin snow is partially transparent thus allowing the observing instrument to “see through” the snowpack) and the amount of contaminants in the upper snow layer, which are dominating factors at the visible reflectances as concluded e.g. by Warren and Wiscombe (1980), Singh et al. (2010) and Dozier et al. (2009). Also, according to these studies, visible reflectance is not sensitive to snow grain size at moderate and coarse grain sizes, which result allowed us to neglect the effect of grain size when investigating the visible spectra in the present study.

Niemi et al. (2012) investigated the behaviour of scene reflectance and found that variation in snow reflectance induced a large variation in the observed scene reflectance, even when canopy covered 48% of

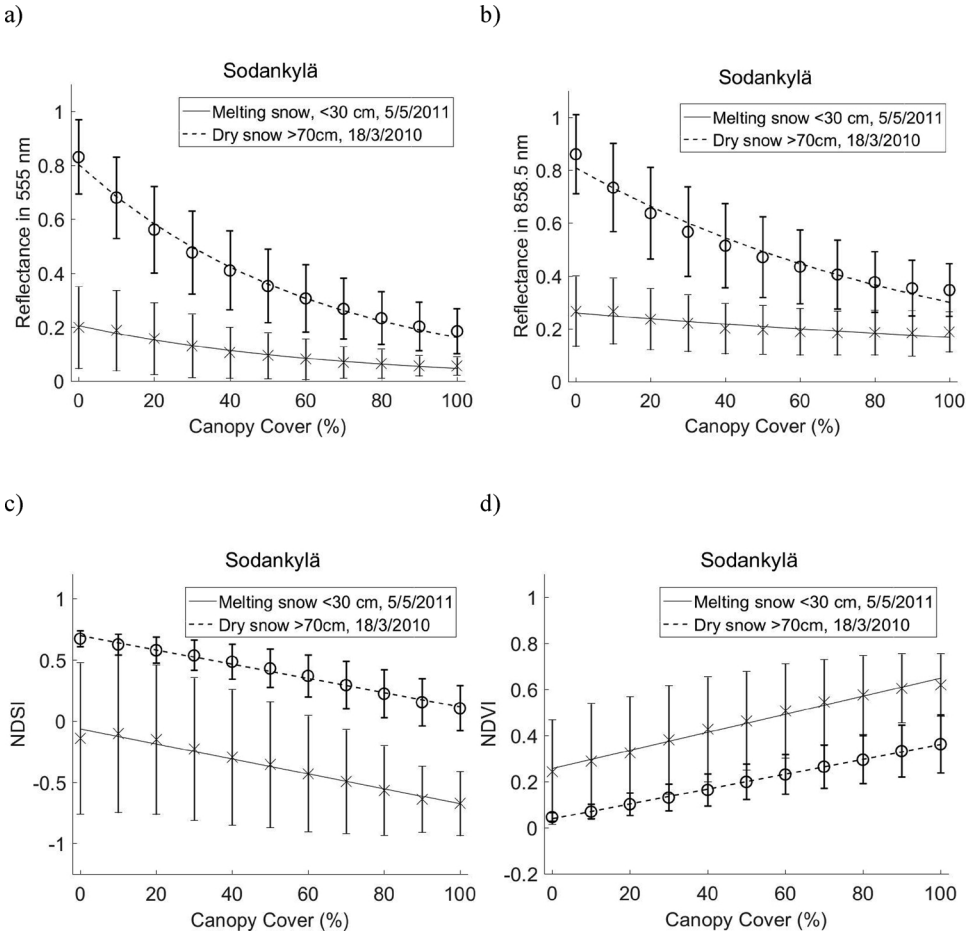

Fig. 5. Mean and standard deviation of thin and thick snow pack at a) green 555 nm reflectance, b) NIR 858.5 nm reflectance, c) NDSI and d) NDVI with respect to Canopy Cover (%) measured in Sodankylä under direct illumination. During the flights on 5 May 2011 the solar elevation θ was 26°–30° and on 18 March 2010 θ was 22°–23°.

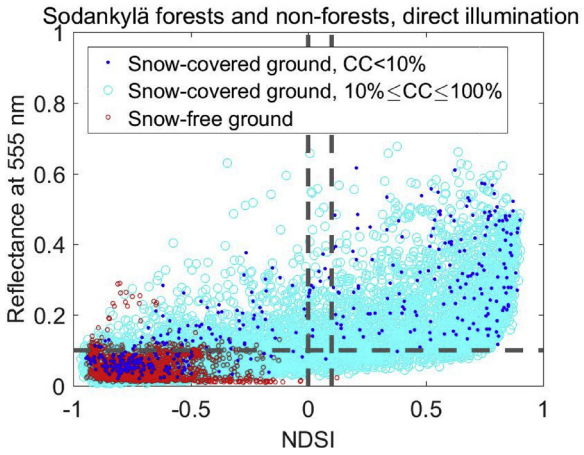

Fig. 6. Scattergram of all AISA observations from the Sodankylä site on 5 May 2011 rectified to 10 × 10 m^2 pixel size showing NDSI in the x-axis and Band 4 (555 nm) reflectance in the y-axis. Observations with snow-covered ground, snow depths < 30 cm, are stratified into two Canopy Cover (CC) categories. Dashed lines represent the thresholds of NDSI and Band 4 in MODIS C6 MOD10_L2 NDSI_Snow_Cover product to identify snow in the pixel.

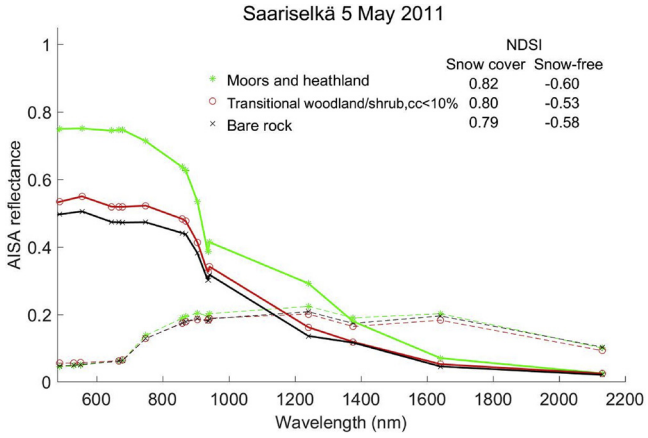

Fig. 7. AISA observations from snow-covered locations, 0 cm < *sd* < 60 cm (solid line) and snow-free locations (dashed line). Observations were made under diffuse illumination in the Saariselkä fell area on 5 May 2011.

the observed scene area. The present study showed similar variation in visible wavelengths (see Fig. 4 and Supplementary Data SD6). However, the most notable relative change between the snow-covered ground and snow-free ground reflectances was observed at 555 nm. This result indicates that the green wavelength region is the most suitable for separating snow cover from the underlying ground during the melting period. This finding is also supported by the results from the utilization of the *SCAmod* method for Fractional Snow Cover (FSC) mapping in boreal forest and tundra obtained by Metsömöki et al. (2012). During the spring melt, the performance of the method is best in non-forested areas where the soil is dark. In forested areas, the method has a high risk to underestimate snow cover.

For snow-covered areas, NDSI was found to fluctuate strongly between the different land cover classes but also inside a single land cover class during the melting period (SD 6). This fluctuation is caused by the contribution of the emerging vegetation underneath the snow pack especially at low snow depths, contaminants on the snow accumulated

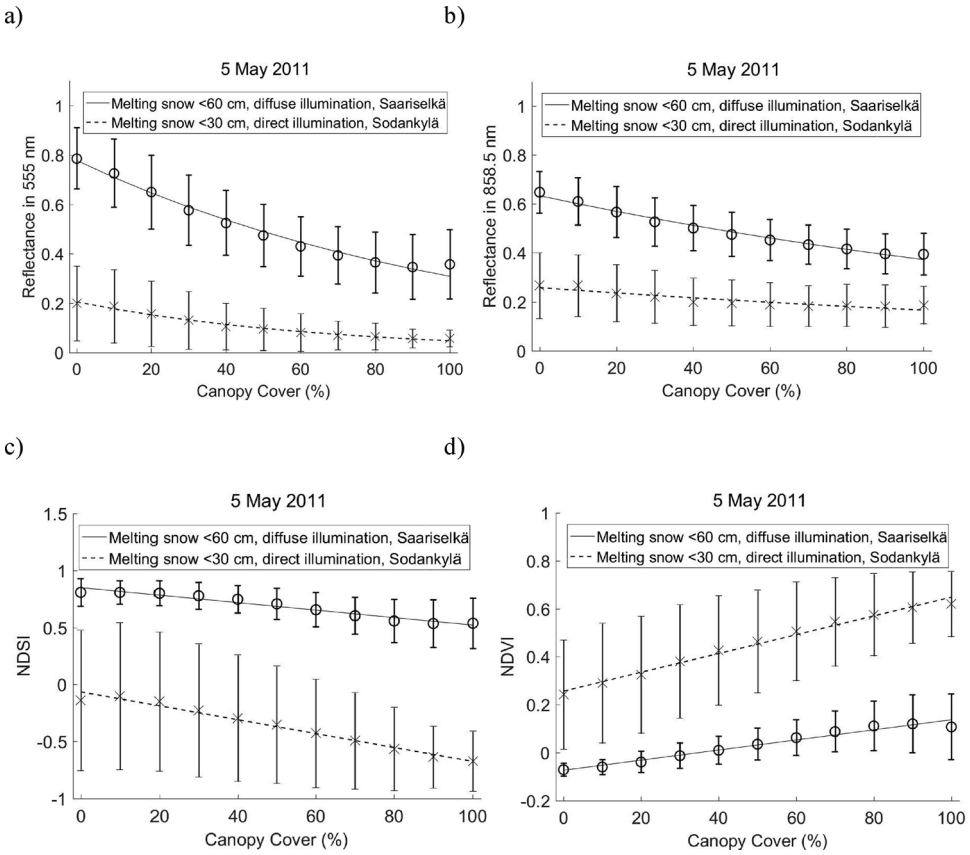

Fig. 8. The mean and standard deviation of a) green reflectance, b) NIR reflectance c) NDSI and d) NDVI, compared with canopy cover (%) in two cases: 1) the ground is covered by a melting snow layer < 60 cm, diffuse illumination and 2) the ground is covered by a melting snow layer < 30 cm, direct illumination.

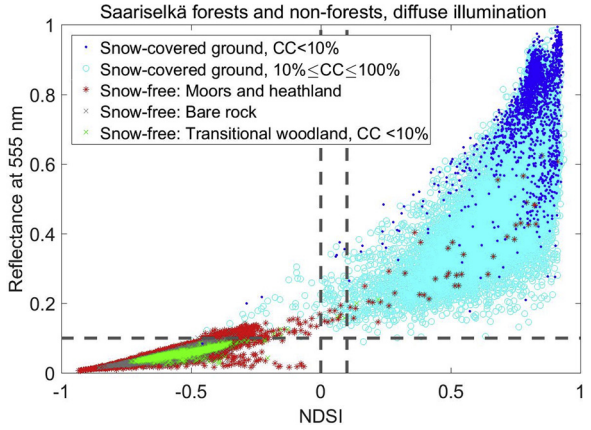

Fig. 9. AISA observations at 10 × 10 m pixel size from the areas covered by melting snow layer, snow depths > 0 cm and < 60 cm, separated into two Canopy Cover (CC) categories and snow-free AISA observations at 80 × 80 cm^2 pixel size from Moors and heathland, Bare rock and Transitional woodland (CC < 10%) from Saariselkä fell area on 5 May 2011 in NDSI − Band 4 space. Dashed lines represent the thresholds of NDSI and Band 4 in MODIS C6 MOD10_L2 NDSI_Snow_Cover product to identify snow in the pixel.

during the melting season as well as by the effect of forest canopy. To find out the effect of Canopy Coverage on this fluctuation we investigated the effect of CC on NDSI under two snow conditions in Sodankylä study site, dry snow with *sd* > 70 cm and melting snow with *sd* < 30 cm. Although the measurement dates and illumination conditions are different, it is of interest to see the differences in the behaviour of the reflectances and indices at the different canopy coverages. We found that standard deviation for NDSI and NDVI are only slightly sensitive to CC when the ground was covered by a dry thick snow layer, while for thin melting snow the variance is in general clearly higher and in addition, more sensitive to CC (Fig. 5). All in all, dry thick snow layer produces higher NDSI and lower NDVI than thin snow layer (see the mean values in Fig. 5c and d). This shows clearly the impact of snow melt heterogeneity on the indices. The variation of NDSI is at least partly due to the stronger effect of viewing and illumination geometry on the SWIR reflectance compared to visible reflectance. Xie et al., 2006 found a strong sensitivity of the bidirectional reflectance to grain size at the NIR/SWIR wavelengths longer than 1.2 μm, while at visible wavelengths there is very slight dependency between bidirectional reflectance and grain size. This reverse behavior causes fluctuation in the NDSI, since NDSI is calculated from visible and SWIR reflectances. Additionally, in late spring the top snow layer contains more impurities e.g. needles, because the impurities pile up to the top snow layer from the melted snow layers above. Also evergreen ground vegetation tends to stick out of the thinning snow layer. Peltoniemi et al. (2005) investigated the spectral and directional reflection properties of the most typical understory types in Finnish forests. They found large differences between species, but there were variations among the samples of the same species too e.g. set of spectra of lingonberry measured at nadir and taken at various locations a few meters apart showed large variations in NIR and SWIR bands. This induces fluctuation to NDSI at the very end of the melting period and indicates the unsteady capability of NDSI-based method for snow detection at that time particularly with space-borne instrumentation for which the bidirectional reflectance effect may be quite remarkable. Heinilä et al. (2014) concluded that even when the Sodankylä study site was covered by dry over 70 cm thick snow layer the NDSI based algorithm could not properly detect snow-covered ground in a forested region. Here we repeated this analysis using two CC categories for NDSI data: CC < 10% and CC ≥ 10% (Fig. 6). We found that the NDSI-based method fails to detect snow also

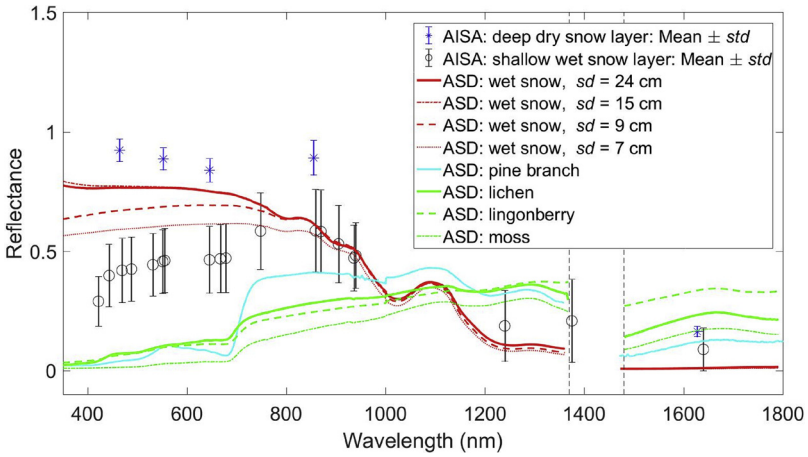

Fig. 10. AISA airborne observations at 80 cm pixel size from under 30 cm thin melting snow layer (black spots), AISA observations at 80 cm pixel size from over 70 cm thick dry snow layer (blue spots) and at-ground ASD observations at surface area of 20 cm in diameter from 7 to 24 cm melting snow layer with grain size of 1 mm (red lines) and vegetation (green lines). Reflectances from pine branch are made at-laboratory condition (cyan line). All observations are made under direct illumination. The wavelengths 1370–1480 nm were disturbed by a bad signal-to-noise ratio (For interpretation of the references to colour in this figure legend, the reader is referred to the web version of this article).

in non-forested areas when snow depth is thin (sd < 30 cm). Fig. 6 also shows the high variation of Band 4 reflectance (555 nm). However, for snow-covered open areas (CC < 10%), the Band 4 reflectance has less < 0.1 values than NDSI (these are the limits for Band 4 and NDSI utilized in C6 NDSI_Snow_Cover to predict snow (Riggs et al., 2016)).

Our investigation showed that the correlation between CC and reflectance at 555 nm is more exponential than linear for thin melting snow layer and especially for dry snow layer (Fig. 5), which supports the utilization of zeroth order radiative transfer equation in snow models in boreal forest region as presented in Pulliainen et al. (2014). Forest canopy also decreases the observable difference between dry snow and melting snow, which difference is noticeable in sparse forests (as trees are not contributing to the observed reflectance. In VIS bands this differences is caused by the variation in snow depth and the amount of contaminants in the upper snow layer as concluded e.g. by Warren and Wiscombe (1980), Singh et al. (2010) and Dozier et al. (2009). In NIR band (859 nm) this difference is due to the sensitivity of NIR reflectance to the grain size as presented in several studies e.g. by Dozier et al. (2009), Nolin and Dozier (2000), Painter et al. (2003), (1998), Singh et al. (2010) and Warren (1982).

Since the sky was cloud-covered during the Saariselkä fell area AISA experiments we had a possibility to investigate the effect of melting snow on AISA reflectance, NDSI and NDVI with minor effect of illumination geometry. We found that visible and NIR reflectances were highest over moors and heathlands (Fig. 7). This is caused by the absence of evergreen vegetation. In contrast to that the mean NDSI was high for all of the three investigated CLC2012 classes having also much lower CV than in Sodankylä study site (sd < 30 cm, direct illumination). The lower variation in NDSI in Saariselkä compared to Sodankylä is at least partly explained by the isotropic illumination conditions, since SWIR reflectance has been found to be sensitive to BRDF in snow-covered conditions (Aoki et al., 2000; Xie et al., 2006). However, the relative change between the reflectance of snow-free and snow-covered ground was highest for all the investigated CLC2012 classes in green wavelengths, which supports the suitability of *SCAmod* snow mapping method for fell areas too.

For melting snow in dense forests during the campaign day in May 2011, the visible reflectances at Saariselkä under diffuse illumination were found to be up to six times higher compared to the observation at Sodankylä under direct illumination (Fig. 8a). This is partially caused by the absence of shadows. However, even in the open areas, where tree-casted shadows are not present, the visible reflectances were notably lower in Sodankylä. We assume that this is mainly due to the thinner snow layer in Sodankylä. Actually the VIS reflectances at Saariselkä were rather close to the Sodankylä dry snow cover reflectances presented in Fig. 5a (sd > 70 cm, direct illumination, March 2010), which is in agreement with the established knowledge on insensitivity of visible reflectance to grain size or liquid water content; e.g. Dozier et al. (2009), Negi et al. (2010), Singh et al. (2010) and Shekhar et al. (2018). Such similarity cannot be found at NIR reflectances when comparing Figs. 8b and 5 b. Importantly, from Fig. 8c we see that for melting snow also NDSI was notably lower in direct illumination in Sodankylä than in diffuse illumination in Saariselkä. In dense forests this NDSI difference was higher than in open areas, which is consistent with the results of Niemi et al. (2012), who obtained much lower NDSI from forest under direct illumination than diffuse illumination. They concluded that both NDSI and NDVI are sensitive to the solar illumination geometry and shadowing caused by the trees. Due to the increasing and stabilizing effect of diffuse illumination on NDSI, the tested MODIS C6 MOD10_L2 NDSI_Snow_Cover criteria detected nearly all of the snow-covered AISA observations from Saariselkä under diffuse illumination (Fig. 9), whereas they failed to do so in the Sodankylä area under direct illumination where spring snow melt was clearly more advanced (Fig. 6).

We also compared the airborne AISA reflectances with the indicative at-ground observed target reflectances. We found that in visible wavelengths, AISA measurements from melting snow layer were notably lower than the ASD measurements from a similar target. In NIR region, the AISA and ASD produced similar values, but in the 1200–1800 nm region the AISA measurements were higher than the ASD measurements. The reflectance of snow itself varies depending on impurities, liquid water content and grain size (Dozier et al., 2009; Grenfell et al., 1981; Hendriks and Pellikka, 2004; Painter et al., 1998; Pellikka and Rees, 2010; Warren, 1982; Warren and Wiscombe, 1980). Overall, compared to the ASD at-ground reflectances from snow the AISA reflectances were closer to the reflectances of vegetation, most likely due to the undergrowth which benetrates to the thin snow layer and the higher amount of impurities on top of the snow layer associated with AISA observations. Also the ASD-observed melting snow contains impurities, but because the original objective of the measurements was to observe the reflectance of a thin melting snow layer in particular, the snow samples included less litter than AISA airborne observations, where the amount of litter could not be controlled. Partly the resemblance of the AISA spectrum to a vegetation spectrum may be caused by the spectrally changing reflection/transmission of the incoming irradiance from/through the trees that surround the observed snow.

The influence of snow depth (sd) on ASD observed reflectance was negligible at values sd = 15 cm and sd = 24 cm, but for sd = 9 cm and sd = 7 cm there was a notable decrease in reflectance of thinning snow observed in the visible region, see Fig. 10. In the NIR region the reflectance was notably lower only at sd = 7 cm. This is due to the dominating effect of the increased effective grain size and the follow-on increased liquid water content of melting snow (Green et al., 2002; Dozier et al., 2009) at NIR in contrast to the dominating effect of contribution of under-laying terrain for shallow snow in visible region (Warren, 1982). Similar results were obtained by Negi et al. (2010):

they investigated the influence of *sd* on spectral reflectance and observed that snow depth affected the reflectance in the visible region and only a minor decrease was observed in wavelengths ≥ NIR region. In their case a significant difference was observed for $sd < 5$ cm. Salminen et al. (2009) also identified a strong effect of *sd* on ASD reflectances. They divided snow depths into two categories, $sd < 20$ cm and $sd > 20$ cm. Their results show a significant reflectance decrease for $sd < 20$ cm. They compared their data with different values of grain size and snow wetness for all snow depths and found that the *sd* was the only factor explaining the behaviour. In addition the above studies, the correlation between the albedo and snow depth is discussed e.g. in Perovich (2007). Although albedo and reflectance are not directly comparable, we surmise we can compare albedo and bidirectional reflectance if not as absolute values then relatively. This is based on e.g. study by Xie et al. (2006) who present how bidirectional reflectance factor is not sensitive to the particle effective size in the visible spectrum and stays slightly below 1. Furthermore, as the ASD measurements with varying snow depths all made within 30 min time frame, under direct illumination and for grain size of 1 mm, the comparison can be made. We found that our results concerning ASD reflectances (Fig. 10) are in line with results by Perovich (2007) as to the dependency of albedo (or reflectance) on the snow depth: according to their study, from approximately 10 cm upwards the depth does not have a noticeable effect on albedo (or reflectance) while a rapid decrease of those quantities with decreasing snow depth occurs at smaller depths.

5. Conclusions

Snowmelt brings challenges to snow mapping during late spring, when snow cover is thin and contains impurities and forest litter. Since information on snow cover extent is particularly important *e.g.* for hydrological and climate modelling near the end of the snow season, studying the spectral behaviour of late spring snow is of great importance. We investigated the behaviour of reflectances and their related indices in different landscapes and illumination conditions during late snowmelt in Finnish Lapland. The acquired AISA (Airborne Imaging Spectrometer for Applications) visible and near-infrared reflectances and NDSI from snow-covered ground were much lower during late spring than during the winter, indicating that the snow melting process has a strong impact on optical wavelengths. We observed that at non-uniform melting snow layer with varying impurities and snow depth causes significant variability and overall decrease especially in visible snow reflectance and NDSI. The coefficients of variation were distinctively high in snow-covered conditions compared to snow-free conditions for all land cover types. The comparison of the Analytical Spectral Devices (ASD) Field Spec Pro JR reflectances from different snow depths in the range of 7–24 cm showed that the effect of snow depth on reflectance is more pronounced in the visible region than in the near-infrared and shortwave infrared region. The ASD and AISA comparison also demonstrated that the adjacent tree canopy (*i.e.* the reflection/transmission of incoming irradiance from/through the trees that surround the observed snow) may affect the reflectance of snow pixel when the instrument measures above the canopy layer.

Overall, reflectance at 555 nm was found to be most efficient in snow detection during the melting period in both the boreal forest region and the fell area, due to its high relative difference between snow-free and snow-covered reflectances compared to other investigated reflectances and indices. This corresponds to the results by Metsömöki et al. (2012) utilizing the *SCAmod* method for Fractional Snow Cover (FSC) mapping in boreal forest and tundra. The comparison of the Canopy Cover and reflectances in direct and diffuse illumination showed that their relation was more exponential than linear in both cases, which supports the utilization of the exponential form of the zeroth order radiative transfer equation in *SCAmod* to describe the effect of canopy on the scene reflectance (Pulliainen et al., 2014). NDSI and NDVI were found to be more applicable in the snow detection under diffuse illumination, since they are very sensitive to illumination conditions and thus their alteration may be caused more by the illumination geometry than by the snow properties This conclusion implies that these indices are at their best with airborne snow mapping since satellite-borne observations can be retrieved only under direct illumination i.e. at clear-sky conditions. Based on the regional data analysis, we also found that NDSI -based snow mapping (based on the high positive NDSI of snow) is more accurate for non-forests than for forests, but at the very end of the melting period the accuracy decreases also in non-forests, since NDSI may have even negative values which are commonly assumed impossible for snow-covered terrain. Although MODIS Collection 6 (C6) NDSI_Snow_Cover product captured less than half of the snow-covered pixels when snow depth was less than 30 cm, the C6 NDSI dataset allows users to generate locally-tuned snow product for various conditions and has thus much potential in snow mapping. Overall, snowmelt has a strong impact on the reflectances and indices, and this fact needs to be considered in the development work of the new improved snow algorithms. Importantly, the sensitivity of NDSI to snow properties and illumination has to be taken into account in the algorithms utilizing the NDSI. Our results can be used especially to refine algorithms used in snow cover mapping, particularly at the end of the melting season.

Acknowledgements

The authors are grateful to the Airborne Imaging Spectroscopy Application and Research on Earth Sciences (AISARES) graduate school of the University of Helsinki, to the Väisälä Fund, to CARBARC project funded by Academy of Finland(285630), to the Spectral Imaging Ltd (SPECIM), as well as to the Joint Center in Earth System Science between College of Global Change and Earth System Science of the Beijing Normal University and Department of Geosciences and Geography of the University of Helsinki for supporting this work.

References

Aoki, T., Fukabori, M., Hachikubo, A., Tachibana, Y., Nishio, F., 2000. Effects of snow physical parameters on spectral albedo and bidirectional reflectance of snow surface. J. Geophys. Res. 105 (D8), 10219–10236. https://doi.org/10.1029/1999JD901122.

Canisius, F., Chen, J.M., 2007. Retrieving forest background reflectance in a boreal region from Multi-angle Imaging SpectroRadiometer (MISR) data. Remote Sens. Environ. 107, 312–321. https://doi.org/10.1016/j.rse.2006.07.023.

Clark, M.P., Hendrikx, J., Slater, A.G., Kavetski, D., Anderson, B., Cullen, N.J., Kerr, T., Örn Hreinsson, E., Woods, R.A., 2011. Representing spatial variability of snow water equivalent in hydrologic and land-surface models: a review. Water Resour. Res. 47, W07539. https://doi.org/10.1029/2011WR010745.

Cohen, J., Lemmetyinen, J., Pulliainen, J., Heinilä, K., Montomoli, F., Seppänen, J., Hallikainen, M.T., 2015. The effect of boreal forest canopy in satellite snow mapping-a multisensor analysis. IEEE Trans. Geosci. Remote Sens. 53, 6593–6607. https://doi.org/10.1109/TGRS.2015.2444422.

Davis, R.E., Hardy, J.P., Ni, W., Woodcock, C., McKenzie, J.C., Jordan, R., Li, X., 1997. Variation of snow cover ablation in the boreal forest: a sensitivity study on the effects of conifer canopy. J. Geophys. Res. 102 (D24), 29389–29395. https://doi.org/10.1029/97JD01335.

Dietz, A.J., Kuenzer, C., Gessner, U., Dech, S., 2012. Remote sensing of snow – a review of available methods. Int. J. Remote Sens. 33, 4094–4134. https://doi.org/10.1080/01431161.2011.640964.

Dozier, J., Green, R.O., Nolin, A.W., Painter, T.H., 2009. Interpretation of snow properties from imaging spectrometry. Remote Sens. Environ. 113, S25–S37. https://doi.org/10.1016/j.rse.2007.07.029.

Frei, A., Tedesco, M., Lee, S., Foster, J., Hall, D.K., Kelly, R., Robinson, D.A., 2012. A review of global satellite-derived snow products. Adv. Space Res. 50, 1007–1029. https://doi.org/10.1016/j.asr.2011.12.021.

Green, R., Dozier, J., Roberts, D., Painter, T., 2002. Spectral snow-reflectance models for grain-size and liquid-water fraction in melting snow for the solar-reflected spectrum. Ann. Glaciol. 34, 71–73. https://doi.org/10.3189/172756402781817987.

Grenfell, T.C., Perovich, D.K., Ogren, J.A., 1981. Spectral albedos of an alpine snowpack. Cold Reg. Sci. Technol. 4, 121–127. https://doi.org/10.1016/0165-232X(81)90016-1.

Hall, D.K., Foster, J.L., Verbyla, D.L., Klein, A.G., Benson, C.S., 1998. Assessment of snow-cover mapping accuracy in a variety of vegetation-cover densities in Central Alaska. Remote Sens. Environ. 66, 129–137. https://doi.org/10.1016/S0034-4257(98)00051-0.

Hassan, Q.S., Sekhon, N., Magai, R., McEachern, P., 2012. Reconstruction of snow water equivalent and snow depth using remote sensing. J. Environ. Inform. 20, 67–74.

https://doi.org/10.3808/jei.201200221.
Heinilä, K., Salminen, M., Pulliainen, J., Cohen, J., Metsämäki, S., Pellikka, P., 2014. The effect of boreal forest canopy to reflectance of snow-covered terrain based on airborne imaging spectrometer observations. Int. J. Appl. Earth Obs. Geoinf. 27, 31–41. https://doi.org/10.1016/j.jag.2013.06.004.
Hendriks, J., Pellikka, P., 2004. Estimation of reflectance from a glacier surface by comparing spectrometer measurements with satellite-derived reflectances. Zeitschrift für Gletscherkunde und Glazialgeologie 38, 139–154.
Härmä, P., Hatunen, S., Törmä, M., Järvenpää, E., Kallio, M., Teiniranta, R., Kiiski, T., Suikkanen, J., 2015. GIO Land Monitoring 2011-2013 in the Framework of Regulation (EU) No 911/2010 - Final Report. January 2015. Finnish Environment Institute. http://www.syke.fi/download/noname/%7BEEEAA343-6236-49F0-9A3E-8FF50ED9D476%7D/107967.
Klein, A.G., Hall, D.K., Riggs, G.A., 1998. Improving snow cover mapping in forests through the use of a canopy reflectance model. Hydrol. Process. 12, 1723–1744. https://doi.org/10.1002/(SICI)1099-1085(199808/09)12:10/11<1723::AID-HYP691>3.0.CO;2-2.
Lin, J., Feng, X., Xiao, P., Li, H., Wang, J., Li, H., 2012. Comparison of snow indexes in estimating snow cover fraction in a Mountainous Area in Northwestern China. Ieee Geosci. Remote. Sens. Lett. 9, 725–729. https://doi.org/10.1109/LGRS.2011.2179634.
Metsämäki, S., Mattila, O.P., Pulliainen, J., Niemi, K., Luojus, K., Böttcher, K., 2012. An optical reflectance model-based method for fractional snow cover mapping applicable to continental scale. Remote Sens. Environ. 123, 508–521. https://doi.org/10.1016/j.rse.2012.04.010.
Metsämäki, S., Pulliainen, J., Salminen, M., Luojus, K., Wiesmann, A., Solberg, R., Böttcher, K., Hiltunen, M., Ripper, E., 2015. Introduction to GlobSnow SE-products with considerations for accuracy assessment. Remote Sens. Environ. 156, 96–108.
Metsämäki, S.J., Anttila, S.T., Huttunen, M.J., Vepsäläinen, J.M., 2005. A feasible method for fractional snow cover mapping in boreal zone based on a reflectance model. Remote Sens. Environ. 95, 77–95. https://doi.org/10.1016/j.rse.2004.11.013.
Molotch, N.P., Barnard, D.M., Burns, S.P., Painter, T.H., 2016. Measuring spatiotemporal variation in snow optical grain size under a subalpine forest canopy using contact spectroscopy. Water Resour. Res. 52, 7513–7522. https://doi.org/10.1002/2016WR018954.
Nagler, T., Bippus, G., Schiller, G.C., Metsämäki, S., Mattila, O.P., Luojus, K., Malnes, E., Solberg, R., Diamandi, A., Larsen, H.E., Wiesmann, A., Gustafsson, D., 2015. CryoLand - Copernicus Service Snow and Land Ice. https://cordis.europa.eu/docs/results/262/262925/final1-20150410-cryoland-no262925-technicalsummary-public.pdf.
Negi, H.S., Singh, S.K., Kulkarni, A.V., Semwal, B.S., 2010. Field-based spectral reflectance measurements of seasonal snow cover in the Indian Himalaya. Int. J. Remote Sens. 31, 2393–2417. https://doi.org/10.1080/01431160903002417.
Niemi, K., Metsämäki, S., Pulliainen, J., Suokanerva, H., Böttcher, K., Leppäranta, M., Pellikka, P., 2012. The behaviour of mast-borne spectra in a snow-covered boreal forest. Remote Sens. Environ. 124, 551–563. https://doi.org/10.1016/j.rse.2012.06.008.
Nolin, A.W., Dozier, J., 2000. A hyperspectral method for remotely sensing the grain size of snow. Remote Sens. Environ. 74, 207–216. https://doi.org/10.1016/S0034-4257(00)00111-5.
Painter, T.H., Dozier, J., Roberts, D.A., Davis, R.E., Green, R.O., 2003. Retrieval of subpixel snow-covered area and grain size from imaging spectrometer data. Remote Sens. Environ. 85, 64–77. https://doi.org/10.1016/S0034-4257(02)00187-6.
Painter, T.H., Roberts, D.A., Green, R.O., Dozier, J., 1998. The effect of grain size on spectral mixture analysis of snow-covered area from AVIRIS data. Remote Sens. Environ. 65, 320–332. https://doi.org/10.1016/S0034-4257(98)00041-8.
Panday, P.K., Williams, C.A., Frey, K.E., Brown, M.E., 2014. Application and evaluation of a snowmelt runoff model in the Tamor River basin, Eastern Himalaya using a Markov Chain Monte Carlo (MCMC) data assimilation approach. Hydrol. Process. 28, 5337–5353. https://doi.org/10.1002/hyp.10005.
Glacier parameters monitored using remote sensing. In: Pellikka, P., Rees, W.G. (Eds.), Remote Sensing of Glaciers - Techniques for Topographic, Spatial and Thematic Mapping of Glaciers. CRC Press, Leiden, pp. 41–66.
Peltoniemi, J.I., Kaasalainen, S., Näränen, J., Rautiainen, M., Stenberg, P., Smolander, H., Smolander, S., Voipio, P., 2005. BRDF measurement of understory vegetation in pine forests: dwarf shrubs, lichen, and moss. Remote Sens. Environ. 94, 343–354.
Perovich, D.K., 2007. Light reflection and transmission by a temperate snow cover. J. Glaciol. 53, 201–210.
Pulliainen, J., Salminen, M., Heinilä, K., Cohen, J., Hannula, H.R., 2014. Semi-empirical modeling of the scene reflectance of snow-covered boreal forest: validation with airborne spectrometer and LIDAR observations. Remote Sens. Environ. 155, 303–311. https://doi.org/10.1016/j.rse.2014.09.004.
Riggs, G.A., Hall, D.K., Román, M.O., 2017. Overview of NASA's MODIS and visible infrared imaging radiometer suite (VIIRS) snow-cover earth system data records. Earth Syst. Sci. Data 9, 765–777. https://doi.org/10.5194/essd-9-765-2017.
Riggs, G.A., Hall, D.K., Román, M.O., 2016. MODIS Snow Products Collection 6 User Guide. http://modis-snow-ice.gsfc.nasa.gov/uploads/C6_MODIS_Snow_User_Guide.pdf.
Riggs, G.A., Hall, D.K., Salomonson, V.V., 2006. MODIS Snow Product User Guide to Collection 5. http://modis-snow-ice.gsfc.nasa.gov/uploads/sug_c5.pdf.
Salminen, M., Pulliainen, J., Metsämäki, S., Kontu, A., Suokanerva, H., 2009. The behaviour of snow and snow-free surface reflectance in boreal forests: implications to the performance of snow covered area monitoring. Remote Sens. Environ. 113, 907–918. https://doi.org/10.1016/j.rse.2008.12.008.
Schwaizer, G., Ripper, E., 2017.). Product User Manual: Snow Cover Extent Collection 500m Continental Europe. Version 1.0. https://land.copernicus.eu/global/sites/cgls.vito.be/files/products/CGLOPS2_PUM_SCE500-CEURO-500m_V1_I1.02.pdf.
Shekhar, C., Negi, H.S., Srivastava, S., 2018. Correlation between effective snow grain size and hyper-spectral absorption peak characteristics – a case study over the North West Himalaya. Remote. Sens. Lett. 9, 1158–1166. https://doi.org/10.1080/2150704X.2018.1516309.
Singh, S., Kulkarni, A., Chaudhary, B., 2010. Hyperspectral analysis of snow reflectance to understand the effects of contamination and grain size. Ann. Glaciol. 51 (54), 83–88. https://doi.org/10.3189/172756410791386535.
Steele, C., Dialesandro, J., James, D., Elias, E., Rango, A., Bleiweiss, M., 2017. Evaluating MODIS snow products for modelling snowmelt runoff: case study of the Rio Grande headwaters. Int. J. Appl. Earth Obs. Geoinf. 63, 234–243. https://doi.org/10.1016/j.jag.2017.08.007.
Törmä, M., Härmä, P., Hatunen, S., Teiniranta, R., Kallio, M., Järvenpää, E., 2011. Change detection for Finnish CORINE land cover classification. In: Michel, U., Civco, D.L. (Eds.), Earth Resources and Environmental Remote Sensing/ GIS Aplications II. SPIE, pp. 14.
Varhola, A., Coops, N.C., Weiler, M., Moore, R.D., 2010. Forest canopy effects on snow accumulation and ablation: an integrative review of empirical results. J. Hydrol. 392, 219–233. https://doi.org/10.1016/j.jhydrol.2010.08.009.
Warren, S.G., 1982. Optical properties of snow. Re. Geophys. Space Phys. 20, 67–89.
Warren, S.G., Wiscombe, W.J., 1980. A model for the spectral albedo of snow. II: snow containing atmospheric aerosols. J. Atmos. Sci. 37, 2734–2745. https://doi.org/10.1175/1520-0469(1980)037<2734:amftsa>2.0.co;2.
Webster, C., Jonas, T., 2018. Influence of canopy shading and snow coverage on effective albedo in a snow-dominated evergreen needleleaf forest. Remote Sens. Environ. 214, 48–58.
Vikhamar, D., Solberg, R., 2003a. Snow-cover mapping in forests by constrained linear spectral unmixing of MODIS data. Remote Sens. Environ. 88, 309–323. https://doi.org/10.1016/j.rse.2003.06.004.
Vikhamar, D., Solberg, R., 2003b. Subpixel mapping of snow cover in forests by optical remote sensing. Remote Sens. Environ. 84, 69–82. https://doi.org/10.1016/S0034-4257(02)00098-6.
Xie, Y., Yang, P., Gao, B.-C., Kattawar, G.W., Mishchenko, M.I., 2006. Effect of ice crystal shape and effective size on snow bidirectional reflectance. J. Quant. Spectrosc. Radiat. Transf. 100, 457–469. https://doi.org/10.1016/j.jqsrt.2005.11.056.
Xin, Q.C., Woodcock, C.E., Liu, J.C., Tan, B., Melloh, R.A., Davis, R.E., 2012. View angle effects on MODIS snow mapping in forests. Remote Sens. Environ. 118, 50–59. https://doi.org/10.1016/j.rse.2011.10.029.